

Demonstration of Brillouin Enhanced Four-Wave Mixing and Phase Conjugation in a Plasma

C. W. Domier and N. C. Luhmann, Jr.

Department of Electrical Engineering, University of California, Los Angeles, California 90024
(Received 22 June 1992)

Brillouin enhanced four-wave mixing and phase conjugation of microwaves in an unmagnetized hydrogen plasma are observed. Transient and steady-state responses of the plasma and the phase conjugate wave are presented. Low-power, low-density operation agrees well with predictions of simple two-fluid plasma theory.

PACS numbers: 52.35.Mw, 42.65.Hw, 52.25.Sw

There has recently been considerable interest [1-4] in generating phase conjugate reflections in plasmas via Brillouin enhanced four-wave mixing (BEFWM). The term "Brillouin enhanced" arises from the enhanced reflectivities generated when the difference frequency between an input signal wave and a pair of antiparallel electromagnetic pump waves is tuned to match a Brillouin resonance (i.e., ion acoustic wave) in the plasma. In this Letter, the first detailed experimental measurements of BEFWM in a plasma are presented, which demonstrate excellent agreement with theoretical expressions for optical mixing and BEFWM under low-power illumination conditions.

BEFWM, in its simplest form, can be modeled as a pair of simultaneous three-wave mixing processes. Consider the situation illustrated in Fig. 1. In the first process, a strong pump wave \mathbf{E}_2 of frequency ω_0 mixes with a weak signal wave \mathbf{E}_s of frequency $\omega_s = \omega_0 + \omega$ to generate a density modulation or "grating" in the plasma. In the second process, another strong pump wave \mathbf{E}_1 of frequency ω_0 (antiparallel to the first) scatters off this grating to generate a phase conjugate wave \mathbf{E}_c of frequency $\omega_c = \omega_0 - \omega$. As the pump intensities are increased, however, this simple model breaks down as the grating formed by \mathbf{E}_1 and \mathbf{E}_c begins to interfere (either constructively or destructively) with the primary grating formed by \mathbf{E}_2 and \mathbf{E}_s .

Simple two-fluid theory suffices to calculate the low-frequency plasma response to the beating of two transverse electromagnetic waves [3]. In the limit of small m/M , the quasineutral steady-state density response is

$$\frac{\tilde{n}}{n_0} = \frac{(m/2M)k^2 \mathbf{v}_1 \cdot \mathbf{v}_2}{(\omega - \mathbf{k} \cdot \mathbf{U}_i)(\omega - \mathbf{k} \cdot \mathbf{U}_i - i\nu_i) - k^2 c_s^2}, \quad (1)$$

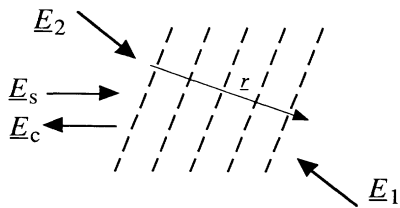


FIG. 1. Four-wave mixing geometry.

where $c_s \equiv [(\gamma_e T_e + \gamma_i T_i)/M]^{1/2}$ is the ion acoustic speed, \mathbf{U}_i is the ion drift velocity, ν_i is the ion damping rate, and $\mathbf{v}_j = e\mathbf{E}_j/m\omega_j$ is the first-order plasma response to the external field \mathbf{E}_j . The density response reaches a maximum when $(\omega - \mathbf{k} \cdot \mathbf{U}_i)^2 = k^2 c_s^2$, at which

$$\frac{\tilde{n}_{\text{res}}}{n_0} = i \frac{m}{2M} \frac{kc_s}{\nu_i} \frac{\mathbf{v}_1 \cdot \mathbf{v}_2}{c_s^2} = i\beta(\mathbf{E}_1 \cdot \mathbf{E}_2), \quad (2)$$

where

$$\beta = \frac{m}{2M} \frac{kc_s}{\nu_i} \left(\frac{e}{m\omega_0 c_s} \right)^2. \quad (3)$$

The quasineutral pulse (step) temporal density response, at resonance, is found to be

$$\tilde{n}_{\text{res}}/n_0 \cong \beta(\mathbf{E}_1 \cdot \mathbf{E}_2)(1 - e^{-\nu_i t/2}) \sin(\omega_{\text{res}} t). \quad (4)$$

Returning to BEFWM, we consider the case where all four electromagnetic waves are polarized parallel to each other (but perpendicular to the interaction plane), and where density grating \tilde{n}_1 , formed by the optical mixing of \mathbf{E}_s and \mathbf{E}_2 , is resonant. Note that this implies that grating \tilde{n}_2 , formed by \mathbf{E}_c and \mathbf{E}_1 , is also resonant. We follow here the approach laid out by Scott and Ridley [5] in their review paper on BEFWM in general (nonplasma) media. The density gratings \tilde{n}_1 and \tilde{n}_2 at resonance are

$$\tilde{n}_1/n_0 = \beta E_2 E_s \sin(kr - \omega t), \quad (5)$$

$$\tilde{n}_2/n_0 = \beta E_1 E_c \sin[(k + \Delta k)r - \omega t],$$

where Δk is the wave-number mismatch between the four waves. Making the usual slowly varying approximation for the electric fields, now expressed in terms of their rms values, we obtain

$$\begin{aligned} \frac{\partial E_1}{\partial r} &= \frac{g}{2} E_c [E_2 E_s \exp(-i\Delta kr) + E_1 E_c], \\ \frac{\partial E_2}{\partial r} &= \frac{g}{2} E_s [E_2 E_s + E_1 E_c \exp(+i\Delta kr)], \\ \frac{\partial E_s}{\partial r} &= \frac{g}{2} E_2 [E_2 E_s + E_1 E_c \exp(+i\Delta kr)], \\ \frac{\partial E_c}{\partial r} &= \frac{g}{2} E_1 [E_2 E_s \exp(-i\Delta kr) + E_1 E_c], \end{aligned} \quad (6)$$

with boundary conditions of $E_1(L) = E_{10}$, $E_2(0) = E_{20}$, $E_s(L) = E_{s0}$, and $E_c(0) = 0$. This set of coupled equations is expressed here in the form utilized by Scott [5], except that the stimulated Brillouin scattering (SBS) gain coefficient g is replaced by its plasma counterpart:

$$g = \frac{\beta \omega_{p0}^2}{k_0 c^2} = \frac{1}{4\pi} \frac{n_0}{n_c} \frac{k c_s}{v_i} \frac{r_e \lambda_0}{M c_s^2}, \quad (7)$$

where $r_e = e^2/mc^2 = 2.82 \times 10^{-13}$ cm.

Equation (6) can be solved analytically under the assumption that the pump waves are much more intense than the signal and conjugate waves, so that we may neglect pump depletion. In the short interaction length limit, where $\Delta k L \ll 1$, we regain the results of Williams, Lininger, and Goldman [3], namely, that

$$\frac{E_c(L)}{E_s(L)} = \frac{E_1 E_2 [e^G - 1]}{E_1^2 + E_2^2 e^G}, \quad (8)$$

where the BEFWM gain coefficient $G = \frac{1}{2} g (E_1^2 + E_2^2) L$. Note that if the signal wave is Stokes shifted ($\omega_s < \omega_0$), rather than anti-Stokes shifted, then g is replaced by $-g$.

Under low-gain conditions, where $|G| \ll 1$, the time response of the conjugate wave E_c to the abrupt turn-on of the pump and/or signal waves is determined predominantly by the time response of the primary grating formed by E_s and E_2 , yielding

$$E_c(t) = \frac{1}{2} g E_1 E_2 E_{s0} L [1 - e^{-v_i t/2}]. \quad (9)$$

The experimental studies are performed in a cylindrical chamber [6] containing an unmagnetized, low-density H_3^+ plasma. Within the chamber are two large lens-corrected microwave horns which launch antiparallel 3.24 GHz pump waves, and a smaller horn which transmits the signal wave and collects the conjugate wave. Because of the $\approx 38^\circ$ tilt angle between the pump and signal waves, both a large- k (formed by E_1 and E_s) and a small- k (formed by E_2 and E_s) grating are created in the plasma. The conjugate wave thus results from the

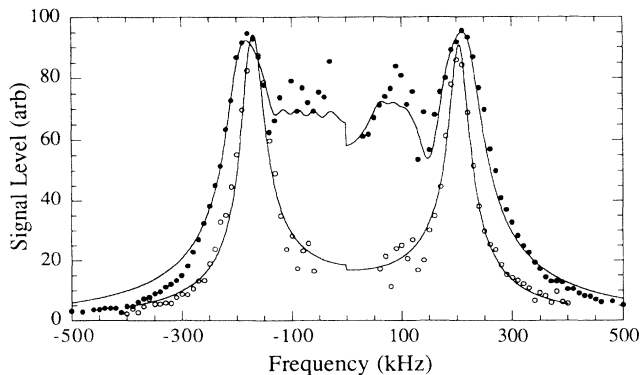


FIG. 2. BEFWM resonances observed from scattering (\circ) and conjugate wave (\bullet) data in an H_3^+ plasma of density $0.18n_c$.

scattering of E_2 off the large- k grating, and of E_1 off the small- k grating.

Figure 2 displays the large- k ion wave (grating) amplitude, obtained by a 38 GHz collective scattering system aligned at a 19° tilt angle, and the conjugate wave amplitude as a function of the difference frequency $f = f_s - f_0$ between the signal and pump waves. The solid lines represent least-squares fits to the data using the frequency response relations of Eq. (1), summed over 28° – 48° for the scattering data and 32° – 76° for the conjugate wave data to account for the range of angles contained within the divergent signal beam. The jump in the fitted responses at $\Delta f = 0$ arises from the fact that the ion acoustic wave (IAW) gratings travel through the plasma at the sound speed c_s . Hence, ion waves observed at one location (and tilt angle) were actually formed at another location (and tilt angle) within the plasma.

The scattering signal data, taken 25 μ sec after the onset of E_1 and E_s , are consistent with $c_s = 1.0 \times 10^6$ cm/sec and $v_i = 220$ kHz. The conjugate wave data, taken at $t = 14$ μ sec under similar conditions, are consistent with $c_s = 1.1 \times 10^6$ cm/sec and $v_i = 290$ kHz. This increased damping rate is a direct result of the close proximity of the signal horn to the interaction region. As ion waves of a particular k traverse from their point of origin, their wave fronts become increasingly misaligned with those being formed locally. This effect can be modeled as a time-varying ion damping rate, given by

$$v_i(t) = v_{i0} + (v_{i\infty} - v_{i0})[1 - e^{-t/t_s}], \quad (10)$$

where v_{i0} is the initial damping rate, $v_{i\infty}$ is the steady-state damping rate, and t_s is the damping rate settling time constant. Provided in Fig. 3 are time histories of the scattering and conjugate wave signals, with $f = +200$ and -190 kHz, respectively, taken from the same data sets as Fig. 2. The data demonstrate excellent agreement

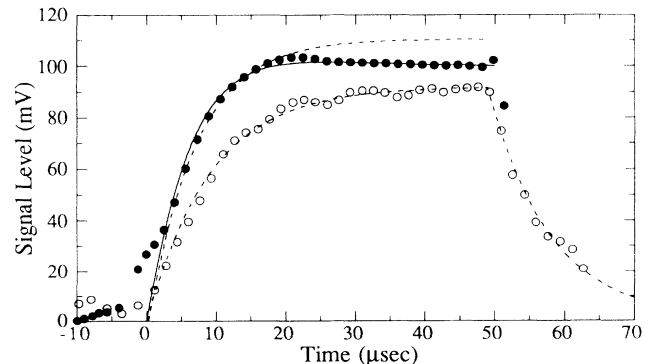


FIG. 3. Scattering signal (\circ), and conjugate wave (\bullet) wave forms at resonance; the dashed lines represent the simple damped responses expected for $v_i = 220$ and 290 kHz, respectively. The solid line represents the conjugate response expected for a time-varying v_i with initial/steady-state values of 220 kHz/ 320 kHz ($t_s = 12$ μ sec).

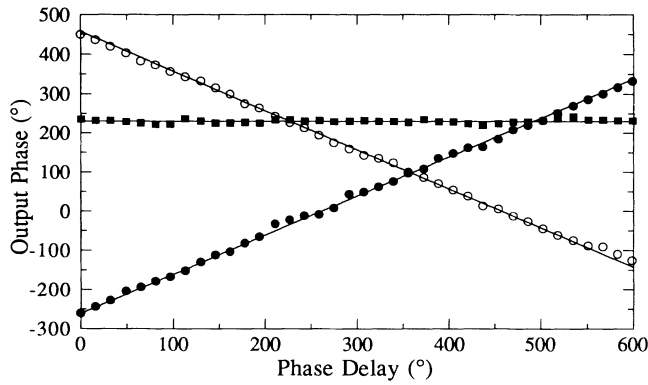


FIG. 4. Conjugate wave phase measurements with a variable phase delay inserted in the signal wave path (O), the conjugate wave path (●), and the path shared by both waves (■).

with Eqs. (4) and (10), as represented by the solid and dashed lines in Fig. 3.

Phase measurements of the output conjugate wave, in which calibrated phase delays were placed along various points in the signal and conjugate wave paths, show in Fig. 4 that the output wave is indeed phase conjugate to the input signal wave. Figure 5 demonstrates that the ion wave and conjugate wave dependence on input pump

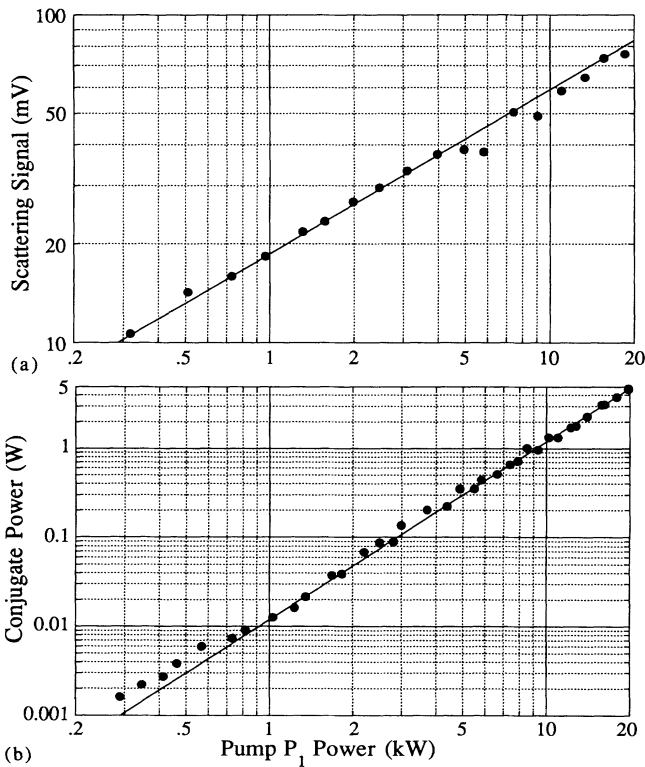


FIG. 5. (a) Scattering signal amplitude ($P_2=0$, $P_s \approx 1120$ W, and $f = +210$ kHz), and (b) conjugate wave power ($P_2 = 0.75P_1$, $P_s \approx 1020$ W, and $f = -190$ kHz), as a function of pump wave power P_1 at time $t = 20 \mu\text{sec}$.

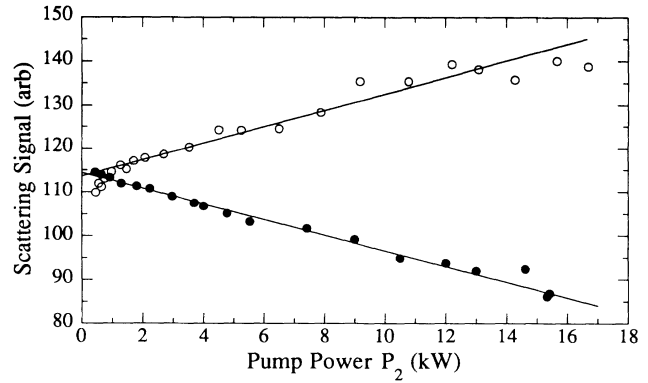


FIG. 6. Scattering signal amplitude as a function of pump wave power P_2 for a 0° tilt angle at time $t = 45 \mu\text{sec}$ with $\Delta f = -190$ kHz (O) and $\Delta f = +200$ kHz (●).

wave power agrees with theory. In order to confirm that the conjugate power observed is the product of a true four-wave interaction, and not solely the product of a three-wave optical mixing process followed by a three-wave scattering process, additional power scaling measurements were taken to determine the large- k ion wave (formed primarily by the mixing of E_1 and E_s) dependence upon pump E_2 . Assuming the conjugate wave is adequately described by Eq. (9), the total steady-state optical mixing generated ion wave is given by

$$\tilde{n}/n_0 = i\beta E_1 E_s (1 \pm \frac{1}{2} g I_2 L), \quad (11)$$

where here $L \approx 90$ cm is the distance from the end of the interaction region to the point of observation (i.e., the location of the scattering beam). With on-axis pump and signal wave intensities of $I_1 \approx 23.0$ kW/2550 cm², $I_2 \approx P_2/720$ cm², and $I_s \approx 1210$ W/720 cm², the SBS gain coefficient g , assuming $v_i = 180$ kHz and $c_s = 9.4 \times 10^5$ cm/sec, is $\approx 2.6 \times 10^{-4}$ cm/W. Substitution of these parameters into Eq. (11) yields the solid lines in Fig. 6, providing an excellent fit to the data points.

Figure 7 presents the conjugate wave plasma density dependence with power levels of $P_1 = 10$ kW, $P_2 = 7.5$

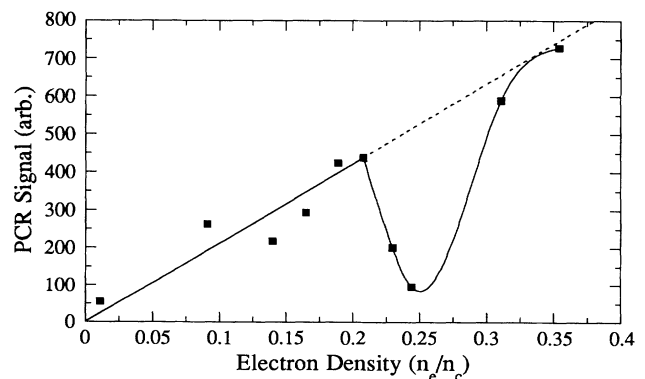


FIG. 7. Conjugate wave amplitude ($\Delta f = -180$ kHz) as a function of plasma density.

kW, and $P_s = 1.2$ kW. The conjugate wave amplitude is seen to deviate from linearity near $0.25n_c$, disrupted possibly by the large amplitude ion fluctuations often observed in the presence of the $2\omega_{pe}$ instability [7] (calculated single pump threshold ≈ 4.3 kW).

In conclusion, BEFWM and phase conjugation in a plasma have been clearly demonstrated. Detailed optical mixing and BEFWM measurements have been found to agree with simple two-fluid theory under low-intensity, low-gain conditions.

This work was supported by the LLNL Laser Fusion Program. The authors acknowledge informative conversations with E. Williams and M. Goldman.

[1] I. Nebenzahl, A. Ron, D. Tzach, and N. Rostoker, Phys.

Fluids **31**, 2144 (1988).

[2] T. Lehner, Phys. Scr. **39**, 595 (1989).

[3] E. Williams, D. Lininger, and M. Goldman, Phys. Fluids **B 1**, 1561 (1989).

[4] M. Goldman and E. A. Williams, Phys. Fluids **B 3**, 751 (1991).

[5] A. M. Scott, Opt. Commun. **45**, 127 (1983); A. M. Scott and M. S. Hazell, IEEE J. Quantum Electron. **22**, 1248 (1986); A. M. Scott and K. D. Ridley, IEEE J. Quantum Electron. **25**, 438 (1988).

[6] H. E. Huey, A. Mase, N. C. Luhmann, Jr., W. F. DiVergilio, and J. J. Thomson, Phys. Rev. Lett. **45**, 795 (1980); C. J. Pawley, H. E. Huey, and N. C. Luhmann, Jr., Phys. Rev. Lett. **49**, 877 (1982).

[7] A. B. Langdon, B. F. Lasinski, and W. L. Kruer, Phys. Rev. Lett. **43**, 133 (1979).